

COMPUTED TOMOGRAPHY AND MAGNETIC RESONANCE IMAGING OF NORMAL CAPRINE MALE GENITAL ORGANS

BY

ABUZAIID, S.M. AND ABUZAIID, R.M.

Department of Anatomy and Embryology, Fac. Vet. Med., Suez Canal University

ABSTRACT

Five adult anesthetized bucks weighing 20-30 Kg were used for the present study. The male genital organs of the buck as identified in computed tomography (CT) and magnetic resonance (MRI) cross sectional images included testes and epididymis (situated outside the pelvic cavity) and vesicular glands, pelvic urethra and bulbourethral glands (situated inside the pelvic cavity). The male organ of copulation, penis, could be identified into three parts (root, sigmoid flexure and free part including the glans).

Although CT images showed superior soft tissue differentiation, T1-weighted MRI images provided greatest contrast and best anatomical details of the male genital organs and was more challenging than computed tomography.

Anatomical features of CT and MRI images were compared with gross anatomical sections to assist in the accurate identification of the specific structures.

INTRODUCTION

Fike, LeCouteur and Cann (1981) introduced Computed tomography (CT) into veterinary medicine to delineate cranial structures. On the other hand, Kraft, Gavin, Wendling and Reddy (1989) did the first publication on sectional imaging by magnetic resonance imaging (MRI) in the veterinary medicine on the brain of the dog. Now, CT has become widely used in dogs and cats (George and Smallwood, 1992; Smallwood and George, 1993; Walker, Hartsfield, Matthews, White, Slater and Thoos, 1993; Jones, Cartee and Bartels, 1995; Drost, Berry and Fisher, 1996; Feene, Evers, Fletcher, Hardy and wallace, 1996; Assheuer and Sager, 1997 and Yamazoe, Ohashi, Kadosawa, Nishimura, Sasaki and Takeuchi, 1999). However, MRI is still used in small scale in veterinary practice (Morgan, Daniel and Donnell, 1994; Hudson, Cauzinille, Kornegay and Tompkins, 1995; Karkkainan, 1995 and Assheuer and Sager, 1997).

Among the goat, very little was written about CT (Smallwood and Healey, 1982; Abuzaid, 1995; and El Hendy, 1999) and MRI (Abuzaid, 1995 and Abuzaid, Suganuma, Al Nahla, Abd EL Tawab and Abuzaid, 1999).

The purpose of the present work was to produce a comprehensive anatomic study of the male genital organs of the buck by CT, MRI and gross anatomical images as essential approach, which has direct clinical relevance in veterinary practice.

MATERIAL AND METHODS

Five adult bucks weighing 20-30 Kg were used in the current study.

For CT, The animals were anesthetized with Halothan® and the pelvis was scanned while the animals were in recumbent position using xpeed TSX-001A (2B 201-134E*F) Toshiba CT scanner. The animals were scanned at 120Kv, 300mAs, 2.7second scan time with window width set at 40. Serial slices of 10mm thickness were done starting from the pelvic inlet and backward up to the level of the ischial arch.

For MRI, the same animals were sedated by Xylaxine® and scanned with Toshiba MRI 50A/III supervision at 35cm field of view and size matrix S192D or 224D (double matrix). Transverse slices of the pelvis were done at 10mm slice thickness, spin echo (SE) pulse sequence image, repetition time (TR) 400-580ms and echo delay time (TE) 15ms.

For gross anatomy, the animals were sedated, well bleed via the common carotid artery and kept in the deep freezer for 48hs. By using slicing machine, transverse slices of 20mm thickness were done from the level of the pelvic inlet till the ischial arch and photographed.

RESULTS

Computed tomography (CT)

Sequential CT scanning of the pelvis of the buck revealed clear anatomical picture regarding the size, shape, position, relation and density of the male genital organs (testes, epididymis, spermatic cord, vesicular glands, urethra, bulbourethral glands and male organ of copulation). The testes, epididymis, vesicular glands and bulbourethral glands showed homogenous soft tissue density. The urethra had a hypodense lumen surrounded by soft tissue density wall and urethral muscle. The male organ of copulation, penis, appeared moderately dense due to its fibrous nature.

At cranial pelvis (fig. 1), the rectum and urinary bladder occupied nearly the whole pelvic cavity. The rectum showed folded wall surrounding a hypodense lumen. The bladder appeared circular with hypo-dense interior due to filling with urine.

About the mid-pelvis (fig. 2&3), the vesicular glands could be easily recognized on the dorsolateral aspect of the pelvic urethra.

Further caudad (fig. 4&5); both testicles, epididymis and spermatic cord were clear outside the pelvic cavity. The spermatic cord could be followed within the inguinal canal, depending on the scanning level and angle.

The penis was seen throughout all the slices of the pelvis scan either as single (free part and root) or double (sigmoid flexure) sections.

Magnetic resonance imaging (MRI)

Further caudad (fig. 4&5); both testicles, epididymis and spermatic cord were clear outside the pelvic cavity. The spermatic cord could be followed within the inguinal canal, depending on the scanning level and angle.

The penis was seen throughout all the slices of the pelvis scan either as single (free part and root) or double (sigmoid flexure) sections.

Magnetic resonance imaging (MRI)

At the internal pelvic aperture (fig.6), the rectum, urinary bladder and colon could be distinguished. The rectum had irregular circular wall and dark lumen. The latter might be contained bright fecal pellets. The urinary bladder appeared circular in outlines with dark lumen (low signal intensity) due to its urine contents. The colon appeared folded with dark interior containing small bright fecal pellets.

Further caudad (fig.7), the vesicular glands could be traced dorolateral to the pelvic urethra as medium signal intensity.

At the mid-pelvis (fig.8), and in addition to the rectum, vesicular glands and urethra, the testes, epididymis and spermatic cord could be easily recognized. Further caudad (fig.9), the spermatic cord could be traced within the inguinal canal.

About the level of the ischial arch (fig.10), the bulbourethral glands could be recognized lateral to the urethra as medium signal intense structures.

The male organ of copulation, penis, was cleared in various sections.

The size, shape, position and shape of various male genital organs were varied according to the scanning level.

Both computed tomography (CT) and magnetic resonance imaging (MRI) demonstrated typical anatomical picture of the male genital organs as revealed in gross sectional images (fig. 11-16).

DISCUSSION

Similar to that mentioned by George and Smallwood (1992), Smallwood and George (1993), Abuzaid (1995), Abuzaid et al (1999) and EL Handy (1999), the CT and MRI slices in the present study were done transverse to the body axis while the animals were placed in ventral recumbence position. Assheuer and Sager (1997) reported that sagittal and dorsal slice directions may be also useful.

In the current work, 10mm slice thickness was used to identify the genital organs of the buck though the modern scanning techniques allow a slice thickness of 1mm which is important in dealing with small lesions. In this connection, Assheuer and sager (1997) demonstrated that the using of small slice thickness requires long scan time that results in high doses of anesthesia and radiation. Moreover, the genital organs of the buck were clearly identified by CT and MRI without using contrast media. However, Assheuer and Sager (1997) mentioned that administration of a radio-dense contrast media for CT examination may be useful to differentiate organs of digestive tract from those of genital system. They added that the use of intravenous contrast increase the sensitivity of MRI examination in pathological cases.

It is worthy to mention that the differences in shape, size and position of the genital organs in both CT and MRI slices were due to the fact that such slices were obtained by scanning different animals at different times. Otherwise, the using of larger physical slice thickness (20mm) increase the difference between them and those of the CT and MRI although they reflect more or less similar anatomical picture. In this respect, EL Handy

(1999) mentioned that using thinner physical slices facilitate image interpretation, since it allows the reader to more readily follow a questioned organ from one slice to another.

REFERENCES

- Abuzaid, R.M. (1995):** Radio- and sonographic anatomical studies on the goat. Ph.D. thesis, Veterinary Medicine, Suez Canal University.
- Abuzaid, S.M.; Suganuma, T., AL Nahla, S.M.; Abd EL Tawab, M. and Abuzaid, R.M. (1999):** Cross sectional anatomy of the abdomen of the goat by computed tomography (CT), magnetic resonance imaging (MRI) and gross anatomy (GA). Summer AAVA meeting, July 7-9, Baton Rouge, Louisiana, USA
- Assheuer, J. and Sager, M. (1997):** MRI and CT atlas of the dog. Blakwell Wissenschaft Berlin, Vienna.
- Drost,W.T.; Berry, C.R. and Fisher, P.E. (1996):** Computed tomography appearance of a normal variant of the canine tentorium cerebelli osseum. *Veterinary radiology and ultrasound*, 37(5) 351-353.
- EL Handy, F.A.O. (1999):** Modern educational technology in teaching veterinary anatomy with special references to applications in practice. Ph.D. thesis, Veterinary Medicine, Cairo University.
- Feeney, D.A.; Evers, P.; Fletcher, T.F.; Hardy, R.M. and Wallace, L.J. (1996):** Computed tomography of the normal canine lumbosacral spine: a morphological perspective. *Veterinary radiology and ultrasound*, 37 (5) 399-411.
- Fike, S.R.; LeCouteur, R.A. and Cann, C.E. (1981):** Anatomy of the canine brain using high resolution computed tomography. *Veterinary radiology*, 22, 236-243.
- George, T.F II and Smallwood, J. E. (1992):** Anatomical atlas for computed tomography in the mesaticephalic dog: Head and neck. *Veterinary radiology and ultrasound*, 33 (4) 217-240.
- Hudson, L.C.; Cauzinille, L.; Kornegay, J.N. and Tompkins, M.B. (1995):** Magnetic resonance imaging of the normal feline brain. *Veterinary radiology and ultrasound*, 36 (4) 267-275.
- Jones J.C., Cartee, R.E. and Bartels, J.E. (1995):** Computed tomographic anatomy of the canine lumbosacral spine. *Veterinary radiology and ultrasound*, 36 (2) 91-99.
- Karkkainan,M. (1995):** Low- and high- field strength magnetic resonance imaging to evaluate the brain in one normal dog and two dogs with central nervous disease. *Veterinary radiology and ultrasound*, 36 (6) 528-532.
- Kraft, S.L., Gavin, P.R.; Wendling, L.R. and Reddy, V.K. (1989):** Canine brain anatomy on magnetic resonance images. *Veterinary radiology*, 30, 147-158.
- Morgan, R.V.; Daniel, G.B. and Donnel, R.L. (1994):** Magnetic resonance imaging of the normal eye and orbit of the dog and cat. *Veterinary radiology and ultrasound*, 35 (2) 102-108.
- Smallwood, J. E. and George, T.F II (1993):** Anatomical atlas for computed tomography in the mesaticephalic dog: Thorax and cranial abdomen. *Veterinary radiology and ultrasound*, 34 (2) 65-83.

Smallwood, J. E. and George, T.F II (1993): Anatomical atlas for computed tomography in the mesaticephalic dog: caudal abdomen and pelvis. *Veterinary radiology and ultrasound*, 34 (3) 143-167.

Smallwood, J. E. and Healey, W.V. (1982): Computed tomography of the thorax of the adult Nubian goat. *Veterinary radiology*, 23 (4) 135-143.

Walker, M.; Hartsfield, S.; Matthews, N.; White, G.; Slater, M. and Thoos, J. (1993): Computed tomography and blood gas analysis of anesthetized bloodhounds with induced pneumothorax. *Veterinary radiology and ultrasound*, 34 (2) 93-98.

Yamazoe, K.; Ohashi, F.; Kodosawa, T.; Nishimura, R.; Sasaki, N. and Tokeuchi (1994): Computed tomography on renal masses in dogs and cats. *J. Vet. Med. Sci.*, 56 (4) 813-816.

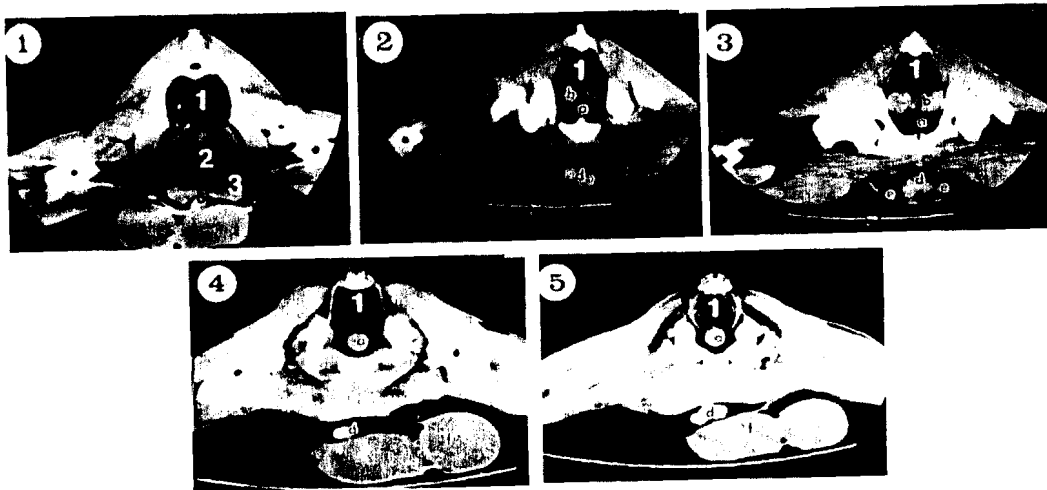


Fig. 1-5: CT step serial transverse sections of the genital organs of the buck at the cranial pelvis (1), mid-pelvis (2&3) and caudal pelvis (4&5).
 1: Rectum; 2: Urinary bladder; 3: Bowel
 a: Urethra; b: Vesicular glands; c: Bulbourethral glands; d: Penis; e: Spermatic cord f: Testes

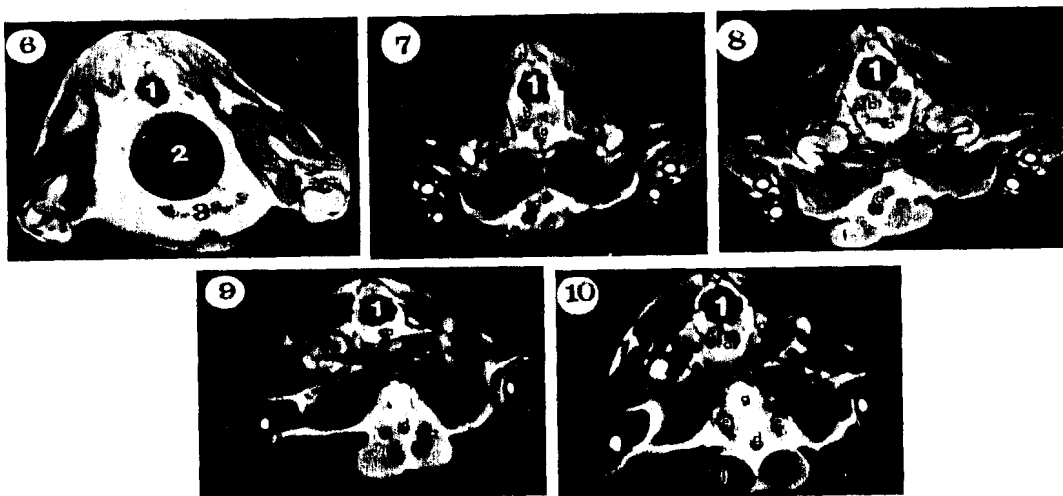


Fig. 6-10: T1-weighted MRI transverse step serial sections of the genital organs of the buck at the pelvic inlet (6), cranial pelvis (7), mid-pelvis (8), caudal pelvis (9) and pelvic outlet (10)
 1: Rectum; 2: Urinary bladder; 3: Bowel
 a: Urethra; b: Vesicular glands; c: Bulbourethral glands; d: Penis; e: Spermatic cord f: Testes; g: Suspensory ligament of the penis

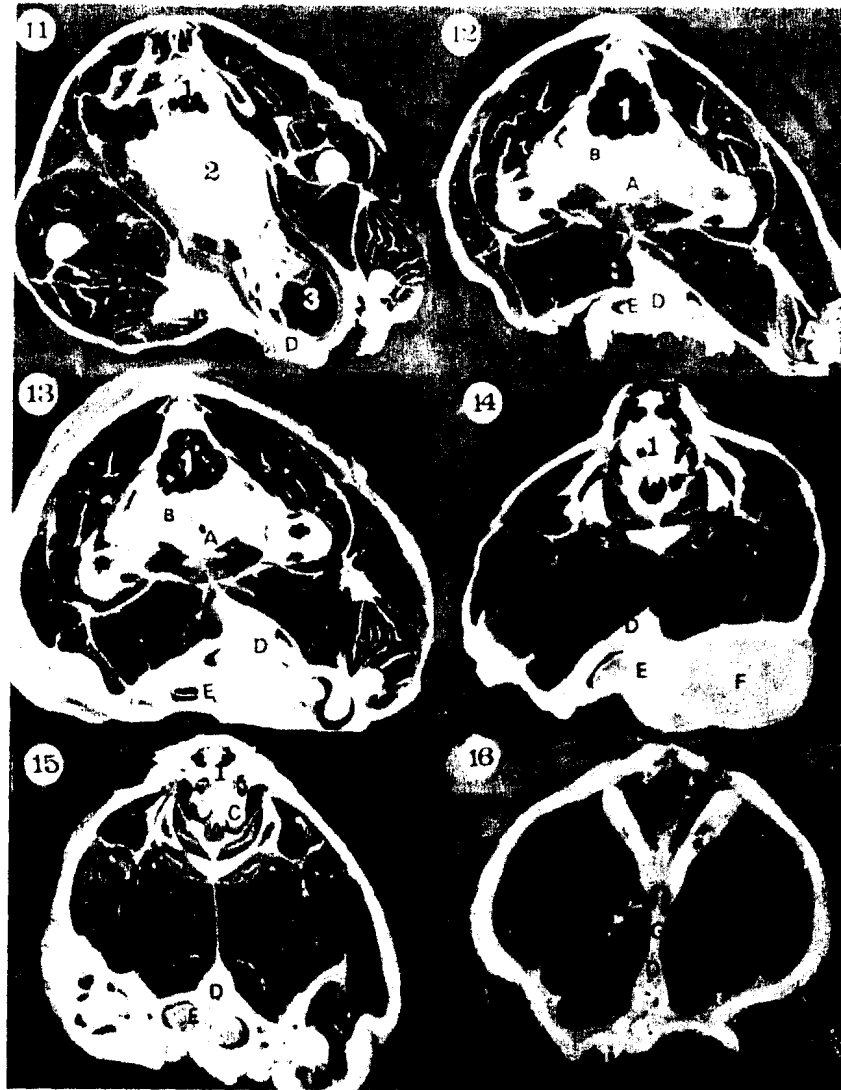


Fig. 11-16: Photographs of serial physical cross sectional anatomy of the pelvis of the buck illustrating the gross anatomy of the male genital organs from the pelvic inlet through its outlet.

1: Rectum; 2: Urinary bladder; 3: Bowel

A: Urethra; B: Vesicular glands; C: Bulbourethral glands; D: Penis;

E: Spermatic cord, F: Testes; G: Suspensory ligament of the penis

الملخص العربي

استخدام التمجرافية المحسوبة وصور الرنين المغناطيسي في توصيف
الأعضاء التناسلية الذكرية السليمة للماعز

صابر محمد شكر أبوزيد و رمضان محمد متولى أبوزيد
قسم التشريح والأجنة ، كلية الطب البيطري ، جامعة قناة السويس

استخدمت في هذه الدراسة خمسة ذكور ماعز تزن ما بين ٢٠-٣٠ كيلوجراماً . وقد اشتملت الأعضاء الذكرية التناسلية للجدي والتي تم التعرف عليها باستخدام التمجرافية المحسوبة وصور الرنين المغناطيسي للقطاعات العرضية على : الخصيتين ، البربخ (متوضعاً خارج التجويف الحوضي) ، وعلى الغدة الحويصلية ، ومجرى البول الحوضي ، وغدة مجرى البول البصلية (متوضعة داخل التجويف الحوضي) . كما تم التعرف أيضاً على الثلاثة أجزاء المكونة للعضو الذكرى التناسلي .

وبالرغم من أن التمجرافية المحسوبة قد أظهرت تمايز الأنسجة الطرية بوضوح ، إلا أن صور الرنين المغناطيسي قد أظهرت التفاصيل التشريحية للجهاز الذكرى التناسلي بتمايز أفضل مما أظهرته التمجرافية المحسوبة .

وقد قورنت كذلك الخصائص التشريحية المتحصل عليها باستخدام التمجرافية المحسوبة ، وصور الرنين المغناطيسي بقطاعات عرضية لعينات تشريحية مجمدة ، وذلك للتثبت من دقة المعلومات المتحصل عليها من الصور .